Research Square

Preprints are preliminary reports that have not undergone peer review.
They should not be considered conclusive, used to inform clinical practice,
or referenced by the media as validated information.

Removal of Sulfur Dioxide by Carbon Impregnated with Triethylenediamine, Using Indigenously Developed Pilot Scale Setup

Sidra Shaoor Kiani (sidrachm5@gmail.com)
Hazara University
Atif Ullah
PIEAS: Pakistan Institute of Engineering and Applied Sciences
Amjad Farooq
PIEAS: Pakistan Institute of Engineering and Applied Sciences
Masroor Ahmad
PIEAS: Pakistan Institute of Engineering and Applied Sciences
Naseem Irfan
PIEAS: Pakistan Institute of Engineering and Applied Sciences
Mohsan Nawaz
Hazara University

Research Article

Keywords: Activated carbon, impregnation, adsorption capacity, challenge gas, breakthrough time, adsorption isotherms

Posted Date: June 17th, 2021

DOI: https://doi.org/10.21203/rs.3.rs-581847/v1

License: This work is licensed under a Creative Commons Attribution 4.0 International License.
Read Full License

Version of Record: A version of this preprint was published at Environmental Science and Pollution Research on January 8th, 2022. See the published version at https://doi.org/10.1007/s11356-021-17653-6.

Removal of Sulfur Dioxide by Carbon Impregnated with Triethylenediamine, Using Indigenously Developed Pilot Scale Setup

Sidra Shaoor Kiani[1,2*], Atif Ullah[1], Amjad Farooq[1], Masroor Ahmad[1], Naseem Irfan[1], Mohsan Nawaz[2]

[1]Hazardous Air Pollutants Laboratory, Pakistan Institute of Engineering & Applied Sciences (PIEAS), Islamabad, Pakistan

[2]Department of Chemistry, Hazara University, Mansehra, Pakistan

ABSTRACT

In order to provide protection against extremely toxic gases Activated Carbon (AC) adsorption has long been regarded to be a useful technology in terms of gas removal. AC without chemical impregnation has been considerably less effective than impregnated ACs. AC in present use was modified with an organic amine i.e. triethylenediamine (TEDA) to enhance the physical and chemical properties of AC in order to remove specific poisonous gases. Purpose of this study was to assess the TEDA impregnated AC in terms of adsorption capability for simulant gas like SO_2. Analysis was done in a properly designed setup. By using the scheme reported here, significant adsorption of toxic gas was obtained. Maximum removal capability observed by AC-4 for SO_2 gas was 3.74 g/g-C and its breakthrough time was 264 minutes. Breakthrough time and adsorption capacity of AC-4 was found to be 25 times and 10 times greater as compared to raw AC. Different characterization techniques were also used to study impregnated AC. It was found that chemical adsorption was the crucial means by which TEDA impregnated AC removed the simulant gas. Langmuir model was best to represent equilibrium and adsorption kinetics follow second order model. The process was endothermic, favorable and spontaneous.

Keywords: Activated carbon, impregnation, adsorption capacity, challenge gas, breakthrough time, adsorption isotherms.

---

*Corresponding author
E-mail: sidrachm5@gmail.com (SS. Kiani)

1. Introduction

Due to high adsorptive properties of AC, it has been employed in a huge range of applications as an easy and safe technique for eliminating contaminants from air stream and from water as well. Of the many carbonaceous materials, activated carbon has gained this special property. This is mainly because of porous nature and huge surface area of activated carbon which makes it functional for removal of irritating and toxic gases from the environment. Impregnating activated carbon (IAC) with warily chosen materials, significantly increases its capacity of adsorption for a large number of gases that raw activated carbon is unable to filter. This marvelous property of activated carbon has been used in the manufacturing of canisters and gas mask filters for the last few decades. With the rising concern on environmental pollution, there has been an increased curiosity in ACs as the means for eliminating pollutants from environment (Abdulrasheed, Jalil et al. 2018, Huve, Ryzhikov et al. 2018, Eskandari, Andalib et al. 2020, Cai, Yang et al. 2021, Wen, Liu et al. 2021). Both the Occupational Safety and Health Administration (OSHA) and Environmental Protection Agency (EPA) have considered AC adsorption as the "gold standard" technology for optimum removal of contaminants on the priority list (Wu, Chang et al. 2007, Yang, Lu et al. 2020).

AC is a nice adsorbent for some organic vapors but for polar and low molecular weight gases, it is a poor adsorbent. On the other hand, impregnated ACs which have been modified with chemical reagent react strongly with these kinds of gases, bind them on the surface and thus remove them from airstream (Ho, Moon et al. 2019, Kiani, Faiz et al. 2020, Kiani, Farooq et al. 2021).

On the AC surface, pollutant gas molecules can be adsorbed by two approaches, physisorption and chemisorption. Physisorption being a surface phenomenon holds the adsorbate pollutant molecules on the surface of AC by Van der Waal's forces and classical electrostatic interactions. In

chemisorption, adsorbent and adsorbate pollutant molecules are held together on AC interface by means of chemical bond. In case of unimpregnated AC, molecules attach to the surface of AC only by weak physical forces. Owing to the weakness of these interactions between adsorbate and AC, adsorbate can be released into atmosphere easily causing several ecological concerns (Mahle, Peterson et al. 2010, Muzarpar, Leman et al. 2020).

Unimpregnated AC does not have the capability to remove contaminants from airstream to a greater extent. Therefore, processes have been developed to coat chemicals on the AC surface to provide essential filtering capabilities. In order to improve removal mechanism of gases from airstream, various treatments were used. Most important one of them is the use of organic coatings (Ho, Chun et al. 2019, Khayan, Anwar et al. 2019). Several impregnating materials i.e. diisopropylamine (DIPA), triethylenediamine (TEDA), piperidine, di-N-propylamine (DNPA), citric acid and tartaric acid have been used for contaminant removal. These "new generation" impregnated ACs can be used for several applications, most important one being used for toxic gases adsorption from air stream. In nuclear testing, most successful combinations to date consist of coal based carbon impregnated with TEDA for the removal of radioactive methyl iodide (González-García, González et al. 2011, Farooq, Irfan et al. 2012, Zhou, Hao et al. 2014, Lee, Lee et al. 2020). In the present work, various types of TEDA impregnated activated carbon samples were prepared by using a very novel and properly developed setup which involves sublimation process for the impregnation of TEDA on activated carbon using Fluidized bed adsorbing tower (FBT). Breakthrough times of IACs were quantified for SO_2 as challenge gases. The intention of present study was to assess the adsorption capacity of AC and TEDA impregnated ACs for SO_2 gas. Concentration of gas was measured by using FTIR based gas analyzer. In addition to IACs, an un-impregnated activated carbon was also tested for gas adsorption capacity.

2. Materials and methods

2.1 Materials/Chemicals

Coal based granular AC having surface area 984 m^2/g, total pore volume 0.423 cm^3/g, density 6.7 g/cm^3, moisture content 11% and pH value of 7.8 was used. Chemical used for impregnation was triethylenedianine ($C_6H_{12}N_2$). Leaching agent used was acetonitrile.

2.2 Design and Scheme of Pilot Scale Impregnation Setup

TEDA was impregnated on AC by using sublimation process. This sublimation process was carried out in a specially designed pilot scale impregnation setup which consists of a fluidized bed adsorbing tower (FBT), TEDA vessel, blower and heat exchanger (HX). These are connected to an electronic control panel (Farooq, Irfan et al. 2012). Design of setup is shown in Fig. 1. Fluidized bed adsorbing tower is the most important part of this setup where TEDA in vapor form impregnates on AC. This technique has the advantage that a uniform impregnant layer can be achieved over all internal and external surfaces of AC.

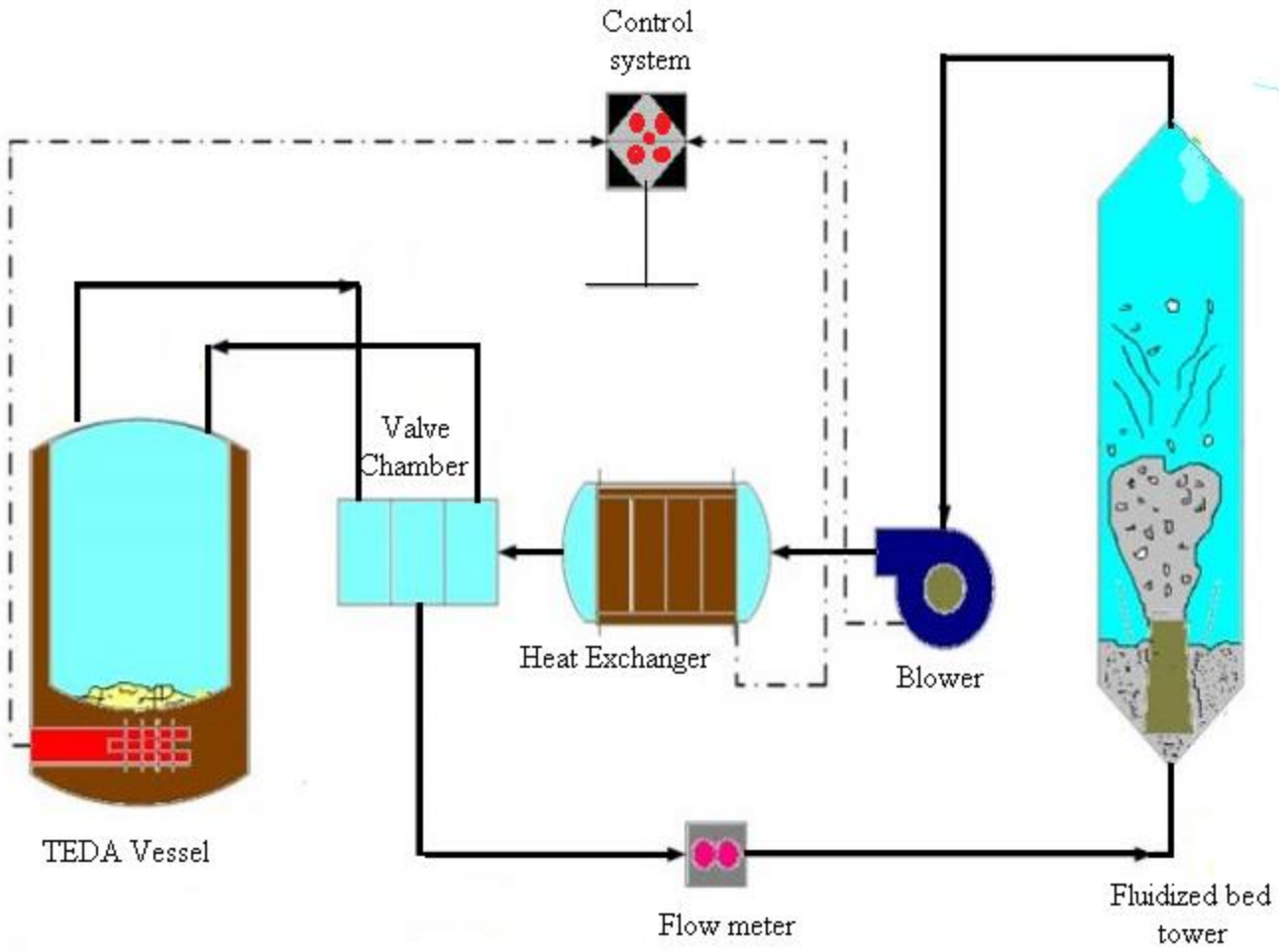

Fig. 1 Experimental setup for TEDA impregnation by sublimation

2.3 Sample Preparation procedure

First of all oil present in the HX is heated by means of heater till it attains 250 °C temperature. Blower is then switched on and air moves towards HX. This hot air then travels directly towards FBT. By this manner, air is recirculated till it attains 100 °C temperature within the FBT. AC bed present inside the FBT is also heated by this hot air. In the meantime, TEDA vessel heater is also operated to attain the temperature of 100 °C for TEDA sublimation. At this time, valve is opened and 100 °C air flows into TEDA vessel, carries TEDA vapors from the vessel and then moves to the FBT. As a result of fluidization of AC bed in FBT, each and every particle of AC from all sides

102 comes in contact with TEDA laden air. So in this manner, TEDA in vapors form gets impregnated
103 on external and internal surfaces of AC. This cycle is repeated for a specified time period until all
104 the TEDA (in the TEDA vessel) is sublimed and gets adsorbed on AC. This method of fluidization
105 and sublimation by using hot air has a number of advantages over other impregnation methods.
106 Here, post drying process of impregnated AC is not needed and this process also ensures uniform
107 impregnation. The samples prepared with various concentration of TEDA are listed in Table 1.

108 Table. 1 Details of TEDA impregnated ACs

Sr. No.	Sample Code	TEDA %	Impregnation temp. (°C)	TEDA vessel temp. (°C)	Activated carbon Amount (kg)	Time (hrs)
1	AC-1	3.2	95	90	2	2
2	AC-2	4	95	90	2	2
3	AC-3	5.5	95	90	2	2
4	AC-4	6.5	95	90	2	2
5	AC-5	7.8	95	90	2	2
6	AC-6	8.5	95	90	2	2
7	AC-7	9.1	95	90	2	2
8	AC-8	10.3	95	90	2	2

109

110 *2.4 Sample characterizations*

111 A Hitachi S-4800 SEM was used to image the samples. Beam extraction current of 15μA,
112 accelerating voltage 20kV and working distance of 12mm were the characteristic conditions
113 employed. To attain stability and to facilitate imaging, a conducting carbon paste for fixing the
114 granules of AC was used. Magnification used was 30-500x.

Determination of breakthrough time was done by FTIR based GASMET Analyzer. For gas filtration, samples were tested by using sulphur dioxide (SO_2) as a challenge gas. 0.5g of each sample was tested for SO_2 gas. These were exposed to 57ppmv challenge gas. Total flow rate comprising SO_2 and diluent N_2 was 3L/min. In dilution chamber, SO_2 gets diluted after mixing with N_2 and passed through AC bed for toxic gas adsorption. Breakthrough time (t_b) was measured as the time when challenge gas concentration downstream of AC bed reached a value of 5ppmv. Experimental setup flow chart for SO_2 testing is shown in Fig. 2.

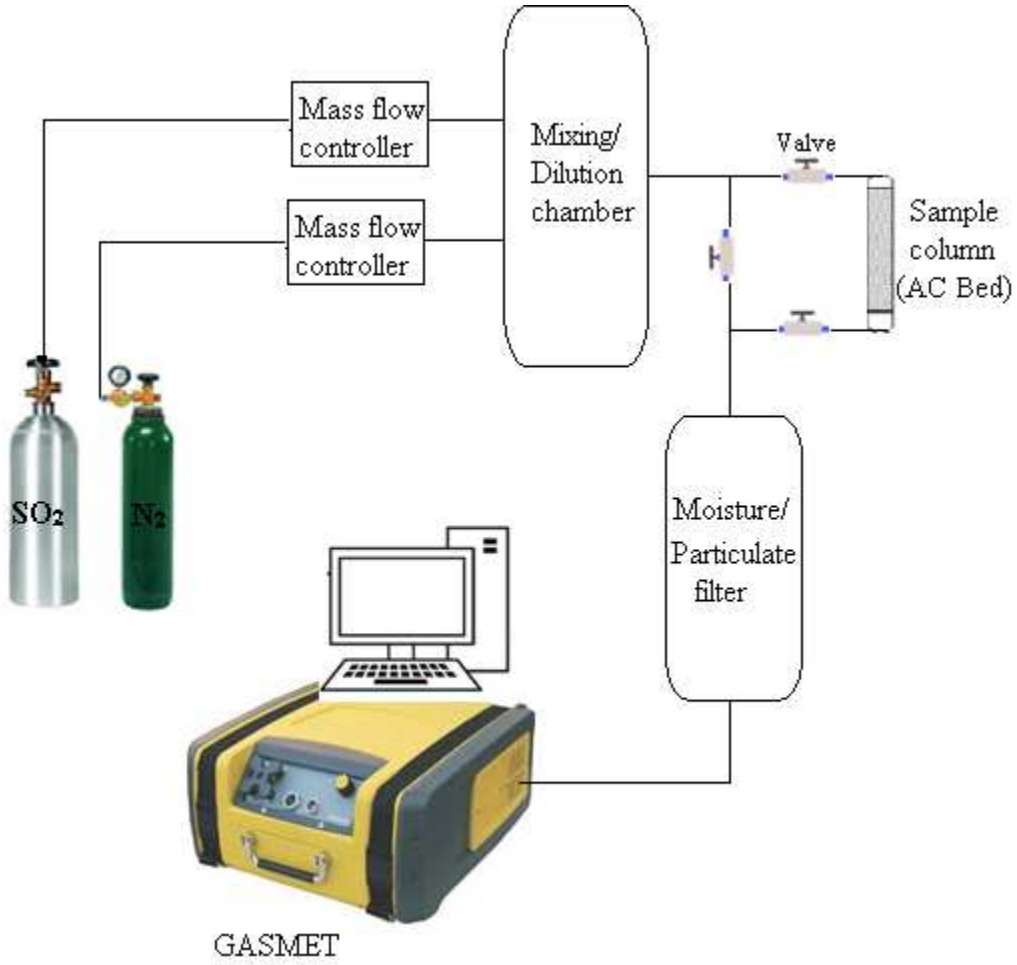

Fig.2 Experimental setup to study SO_2 adsorption on AC

126 *2.5 ASTM Standard Tests for AC*

127 ASTM standard tests were performed to calculate the Particle size distribution, Ball-pan hardness
128 number, Water solubles, Apparent density, Total ash content, Moisture content, Iodine number
129 and pH of Raw and TEDA impregnated activated carbon sample (ASTM 1996).

130 *2.6 Adsorption capacity*

131 Experimentally, adsorption capacity was calculated by using breakthrough time curve data by
132 subtracting the area below the breakthrough time curve from the total area. This final area above
133 the curve gives value of adsorption capacity. Area below breakthrough curve was calculated by
134 integration method. Theoretically, breakthrough time was determined by using modified Wheeler
135 Jonas equation and this equation is written as:

$$\frac{t_x}{t_{0.05}} = 1 - \frac{F}{VK_v}\ln\left(\frac{C_o - C_x}{C_x}\right) \qquad (1)$$

Where, t_x is the breakthrough time (min), $t_{0.05}$ is saturation time (min), F is total flow rate (cm^3/min), V is volume of packed bed (cm^3), K_v is adsorption rate constant (min^{-1}), C_o = inlet gas concentration (gm/cm^3) and C_x is the concentration at time t_x (gm/cm^3).

136 *2.7 Adsorption isotherms*

137 The adsorption data of SO_2 on AC was subjected to three adsorption models i.e. Langmuir,
138 Freundlich and Dubinin-Radushkevich (D-R). Langmuir isotherm was applied in the following
139 linearized form (Lua and Guo 2001):

140 $$\frac{C_e}{C_{ads}} = \frac{1}{Qb} + \frac{C_e}{Q} \qquad (2)$$

141 C_e is the equilibrium concentration of gas (SO_2) in ppm, C_{ads} is the adsorbed concentration of gas
142 on activated carbon in ppm. Q is the constant which signifies maximum adsorption capacity at
143 monolayer formation and b is the characteristic Langmuir constant for the adsorption system.

144 Freundlich adsorption isotherm was applied in the following linearized form (Lua and Guo 2001):

145 $$lnq_e = lnK_f + \frac{1}{n} lnC_e \quad (3)$$

146 q_e is the amount of gas adsorbed, C_e is the equilibrium concentration of gas, K_f is the Freundlich
147 rate constant and $\frac{1}{n}$ is Freundlich adsorption constant strength.

148 D-R adsorption isotherm was applied in the following linearized form (Lua and Guo 2001):

149 $$lnq_e = lnq_s - K_D \mathcal{E}^2 \quad (4)$$

150 Where q_s is the constant in D-R isotherm which is related to adsorption capacity, K_D is constant
151 related to mean free energy of adsorption and $\mathcal{E}$ is the Polanyi potential which is given by:

152 $$\mathcal{E} = RTln(1 + 1/C_e) \quad (5)$$

153 Where R is gas constant, T is absolute temperature and $C_e$is equilibrium concentration of gas.

154 2.8 Adsorption kinetic models

155 Mass transfer phenomenon can be best understood by its thermodynamics and kinetics. Pseudo
156 first order and second order models were applied to analyze the adsorption data for kinetic study.
157 Pseudo first order model is the simplest equation which relates dependence of adsorption rate on
158 adsorption capability. Equation is written as (Sumathi, Bhatia et al. 2010):

159 $$\frac{dq}{dt} = k_1(q_e - q_t) \quad (6)$$

160 Linearized form is given as:

161 $$\log(q_e - q_t) = logq_e - K_1 2.303t \quad (7)$$

162 q_e and q_t are the amounts of gas adsorbed at equilibrium and at time "t" respectively, K_1 is rate
163 constant of pseudo first order and t is contact time.

164 Equation for pseudo second order model is written as:

165 $$\frac{dq}{dt} = K_2 (q_e - q_t)2 \quad (8)$$

166 Linearized form is given as:

167 $$\frac{t}{q_t} = \frac{1}{K_2 q_e} + \frac{t}{q_e} \quad (9)$$

168 Where t is time in min and $^{q}/_{t}$ is the amount of gas adsorbed at time$t$, K_2 is rate constant of pseudo
169 second order reaction and q_e is equilibrium adsorption capacity.

170 2.9 Thermodynamic parameters

171 The primary thermodynamic parameters which are used to calculate the probability and
172 spontaneity of adsorption process are change of enthalpy (ΔH), change of entropy (ΔS) and free
173 energy change (ΔG). Following equations can be used to predict these parameters (Myers 2002):

174 $$\Delta G = -RTlnK_d \quad (10)$$

175 R is gas constant, T is absolute temperature and K_d is distribution coefficient and is calculated by
176 following equation.

177 $$K_\mathrm{d} = (Co{-}Ce)/(ms/V)Ce \quad (11)$$

178 Value of entropy change and enthalpy change was analyzed from intercept and slope of plot
179 between lnK_d verses $^1/_T$ respectively.

180 **3. Results and Discussion**

181 Comparison of ASTM standard test results of Raw AC and AC-4 was made and shown in Table
182 2. Results clearly indicate that AC-4 showed an enhancement in properties as compared to the Raw
183 AC. This is mainly because of the impregnant which imparts these improved properties (Al-Qodah
184 and Shawabkah 2009). So we can say that the prepared AC-4 sample might be a sustainable
185 candidate for purification of noxious gases from atmosphere.

186 Table 2 ASTM standard tests for Raw AC and AC-4

ASTM Standard Tests	Raw AC	AC-4
Mean Particle Size (mm)	0.77	0.88
Ball Pan Hardness Number	91.9	94
Water Solubles (%)	0.01	0.35
Apparent Density (gm/cm^3)	0.41	0.43
Total Ash Content (wt. %)	5	5.5
Moisture Content (wt. %)	19.5	0.85
Iodine Number (mg/g-C)	920	1031
Ph	7.8	9.54

187

188 SEM analysis was done to study the distribution of TEDA on AC surface. Fig. 3 (a) and (b) show
189 SEM images of Raw AC at different magnifications which represent cracks and cavities on surface
190 representing a system of complex porous network. Impregnation results in blocking of cavities and
191 cracks and clogging of pore openings (Kiani, Faiz et al. 2020). Fig. 3(c), (d), (e), (f), (g) and (h)
192 represent the distribution of different concentrations of TEDA on surface of AC-1, AC-3, AC-4,

AC-5, AC-7 and AC-8. In all these images, it can be seen that the AC surface is immensely covered with TEDA impregnants. Better the distribution of TEDA on surface, better will be its capability to react with toxic gases in atmosphere by adsorbing them on the surface of AC by means of chemical bond with the impregnant. Apart from the chemical adsorption of gases on AC, some pores are also available on AC which are responsible for physical adsorption of gases (Wu, Chang et al. 2007, Arcibar-Orozco, Rangel-Mendez et al. 2013). As TEDA is basic in nature, it plays a significant role in the removal of acidic gases like SO_2 from air.

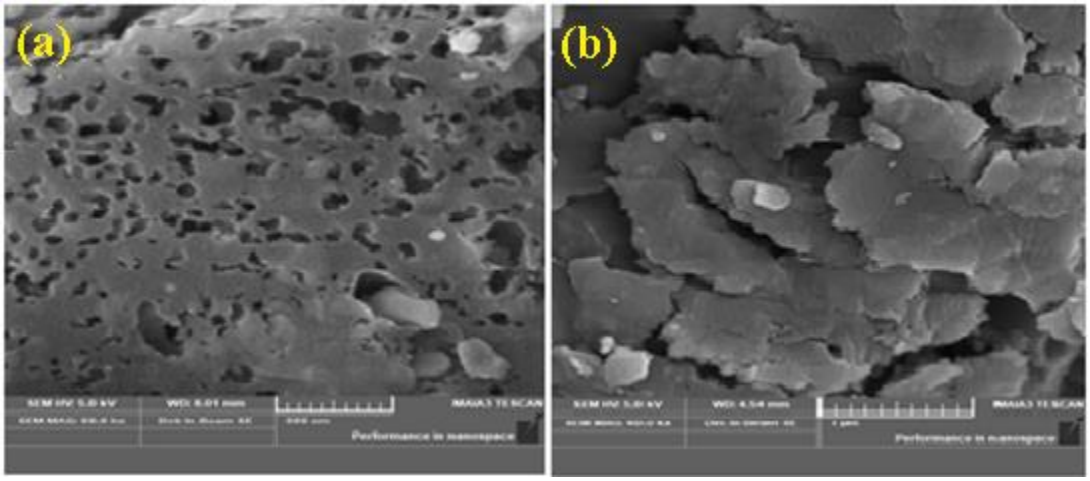

Fig. 3(a) SEM images of Raw AC at (a) 60kx and (b) 50kx

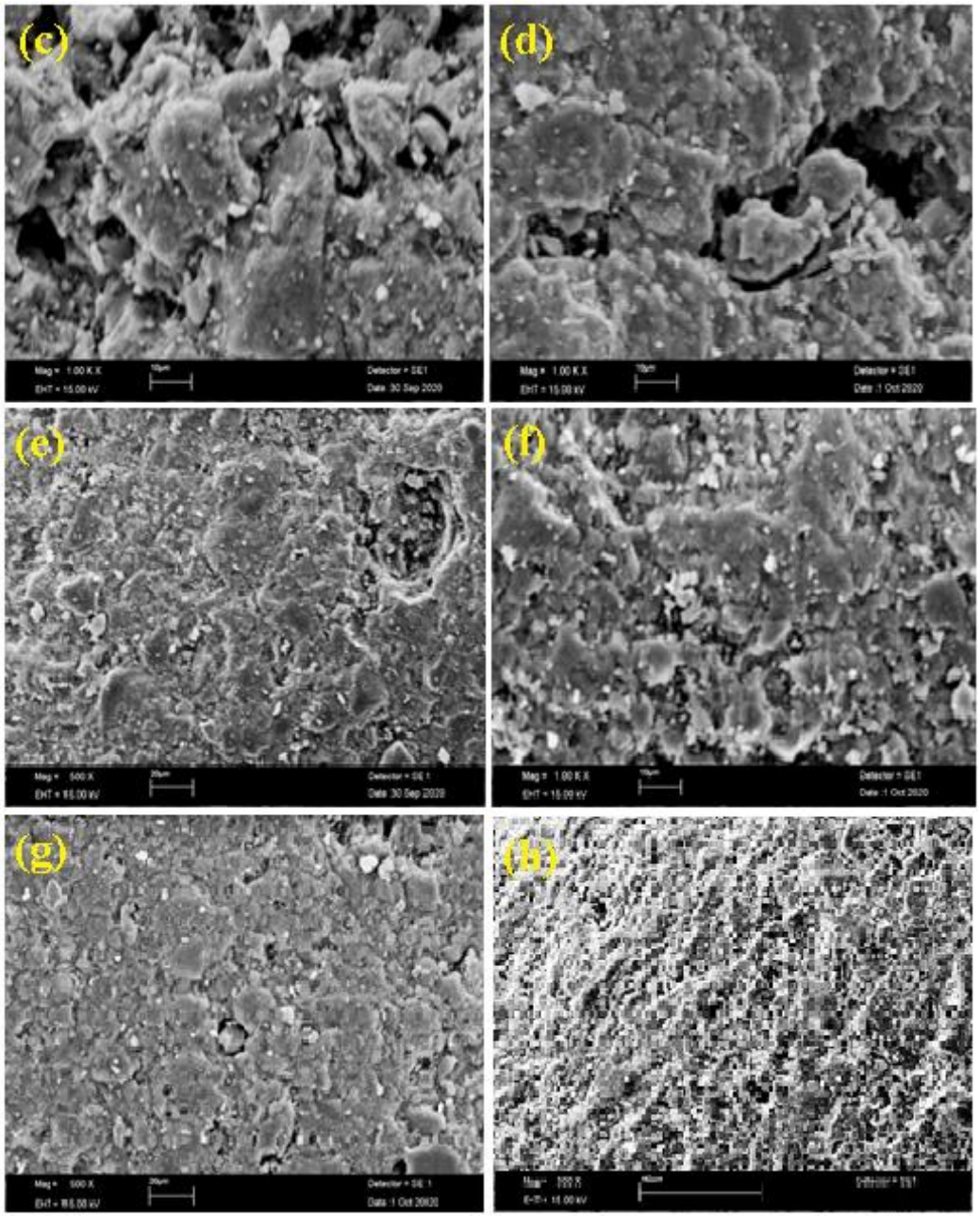

Fig. 3(b) SEM images of impregnated ACs (c): (AC-1), (d): (AC-3), (e): (AC-4), (f): (AC-5), (g): (AC-7) and (h): (AC-8)

pH of samples was measured by ASTM-D3838 method and results are presented in Fig. 4. Results clearly show that as we increase the amount of TEDA, pH value of ACs also increases. This is due to the fact that TEDA is basic in nature and its impregnation makes AC more basic. This increased

basicity of adsorbent (by means of basic adsorbent) is highly desirable for the chemical adsorption of acidic gases as it leads to the filtration of acidic gases from contaminated environment more efficiently (Wu, Chang et al. 2007).

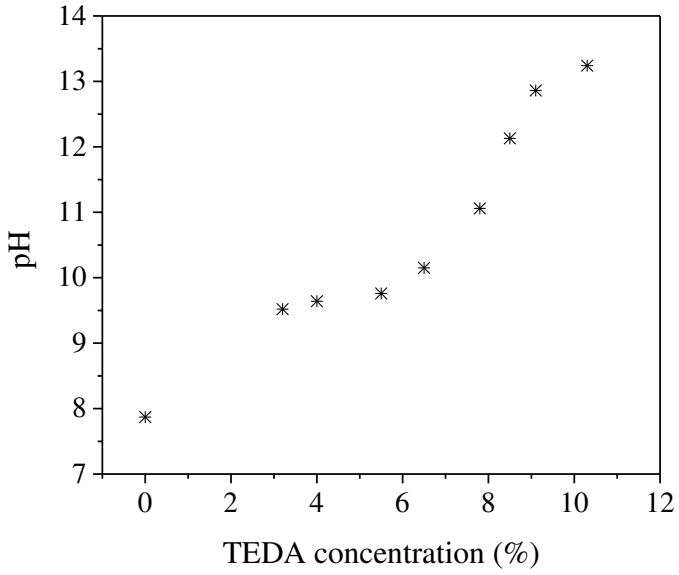

Fig. 4 pH of TEDA impregnated AC samples

Gas filtration capability was tested for SO_2 gas. Comparison of breakthrough time was made between the raw and various TEDA impregnated ACs and shown in Fig. 5(a) and 5(b). These results indicated that Raw AC showed less breakthrough time i.e. 11.6 min as compared to other impregnated samples and so responsible for the purification of toxic gases to lesser extent. In case of TEDA impregnated samples breakthrough time increases initially with the increase in concentration of TEDA but after a certain limit of impregnation, breakthrough time decreases with further increasing the concentration and is shown in Fig. 5(c). The reason behind this is the blocking of pore mouths. Impregnation beyond a certain limit results in the blockage of AC pores and gas molecules do not find more available sites for adsorption, hence its breakthrough time

decreases considerably (Wu, Chang et al. 2007, Bobbitt, Mendonca et al. 2017). After 7% TEDA impregnation, a considerable decrease in breakthrough time was observed. Breakthrough time of AC-1, AC-2, AC-3, AC-4, AC-5, AC-6, AC-7 and AC-8 is 160, 191, 247, 264, 234, 222, 220 and 211 minutes respectively. Breakthrough time of AC-4 is almost 25 times greater than Raw AC. SO_2 adsorption was supposed to occur through subsequent paths (Kiani, Faiz et al. 2020):

For Raw AC: $$AC + SO_2 \rightarrow AC - SO_2 \quad (12)$$

For sample: $$C_6H_{12}N_2 + 2SO_2 \rightarrow SO_2 - NC_6H_{12}N - O_2S \quad (13)$$

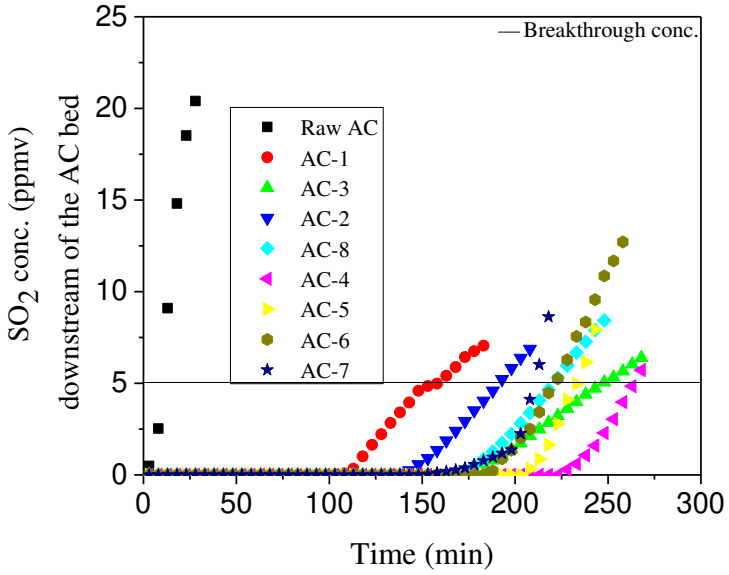

Fig. 5(a) Breakthrough time curves of TEDA impregnated samples for 57 ppmv SO_2 as challenge gas

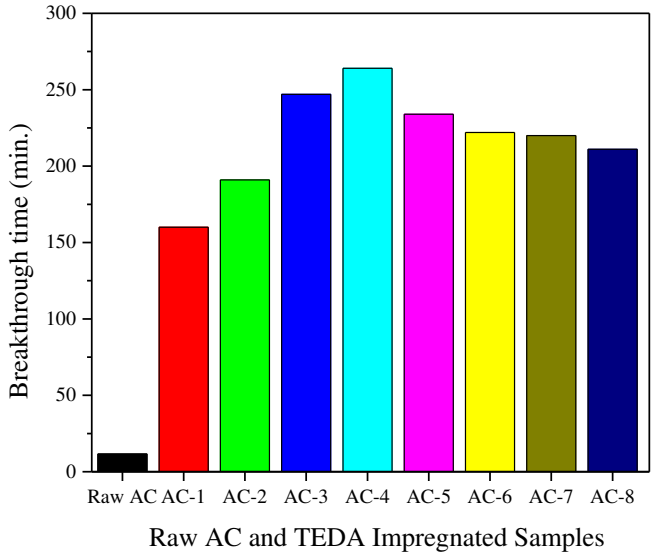

Fig. 5(b) Comparison of breakthrough time of TEDA Impregnated samples (at 5 ppmv) for SO_2 gas

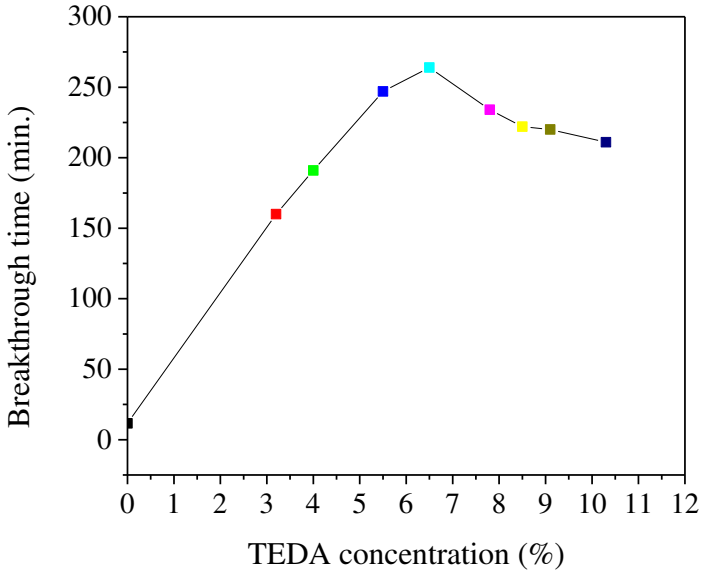

Fig. 5(c) Relation between breakthrough time and TEDA concentration

Adsorption capacity of Raw AC was found to be 0.41 gSO_2/g-C whereas all other impregnated samples showed higher adsorption capacities. Maximum adsorption capacity was observed for

AC-4 which is about 10 times higher than Raw AC as shown in Table. 3. The order of adsorption capacities of samples was found as Raw AC<AC-1<AC-2<AC-8<AC-7<AC-6<AC-3<AC-5<AC-4 for SO_2 gas. Impregnation of TEDA on AC surface might be responsible for a greater resistance or reaction sites (Mahle, Peterson et al. 2010, Perera, Ranjith et al. 2012, Zhou, Su et al. 2018, Hyuncheol Lee 2019).

Table 3 Adsorption capacities of Raw and TEDA impregnated ACs

Sample Code	Adsorption capacity (g SO_2/g-C)
Raw AC	0.41
AC-1	1.98
AC-2	2.54
AC-3	3.18
AC-4	3.74
AC-5	3.48
AC-6	3.10
AC-7	3.04
AC-8	2.97

Table 4 shows breakthrough time of samples calculated by using modified Wheeler Jonas equation. A plot of $\frac{t_x}{t_{0.05}}$ vs $\ln\left(\frac{C_o-C_x}{C_x}\right)$ gives a straight line with slope equal to $\frac{F}{VK_v}$ and intercept 1 (Zhou, Feng et al. 2011). Breakthrough time calculated by this method showed almost the same trend as exhibited by the experimental method, although, the calculated breakthrough times are slightly on higher side as compared to the experimental ones.

Table 4 Breakthrough time by using modified Wheeler Jonas equation

Sample Code	Calculated Breakthrough Time (min.)
Raw AC	18
AC-1	198
AC-2	241
AC-3	264
AC-4	290
AC-5	259
AC-6	277
AC-7	262
AC-8	249

Fig. 6 shows comparison of breakthrough time calculated by both methods. It can be seen that experimental and model results are linearly varying, but the model breakthrough time is slightly greater than experimental breakthrough time (Lodewyckx, Wood et al. 2004). The reason is that theoretical equations always over predict physical quantities. The regression value is 0.97 which shows a good linear fit between model and experimental results.

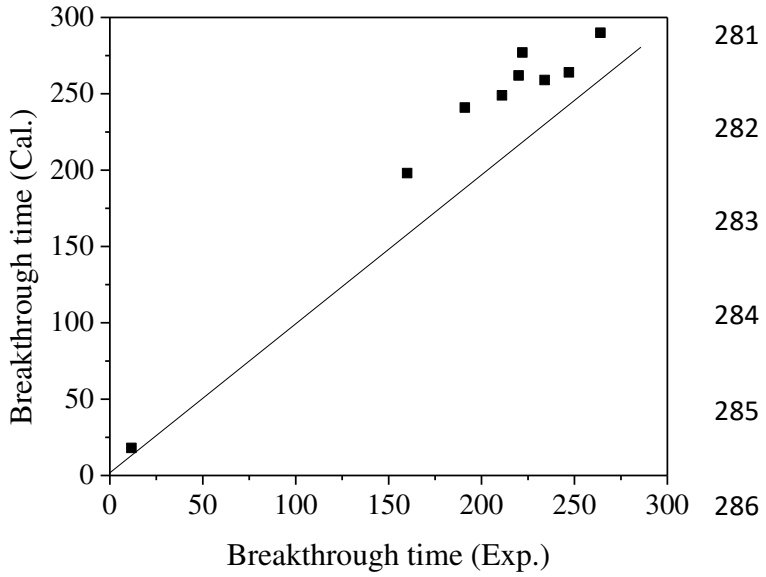

Fig. 6 Plot of Experimental and Model breakthrough time

4. Adsorption isotherms

4.1 Langmuir adsorption isotherm

Fig. 7 shows plot of C_e/C_{ads} vs C_e for SO_2 on AC-4 with initial concentration 57 ppm at 298 K. From the intercept and slope of this plot, values of Langmuir parameters are estimated for the system. Value of R^2 determines the favorability of adsorption process and its corresponding data is given in Table 5. Langmuir isotherm considers that the ions remain adsorbed on certain sites that are mono-energetic and each site binds only one adsorbate molecule without any interaction with the neighboring ions. Moreover, it supports the monolayer adsorption of gas on substrate (Lua and Guo 2001).

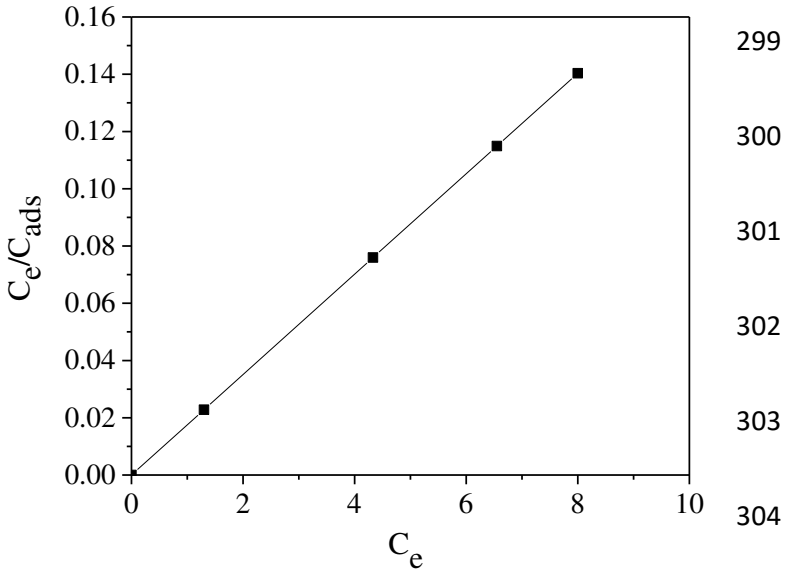

Fig. 7 Langmuir plot of SO_2 adsorption on AC-4

4.2 Freundlich adsorption isotherm

Fig. 8 shows the plot of $\ln C_e$ vs $\ln q_e$ for the adsorption data of SO_2 gas on AC-4 at initial concentration of 57 ppm and 298 K. Slope and intercept were used to determine the Freundlich constant (Muzarpar, Leman et al. 2020). Value of R^2 determines the favorability of adsorption process and its corresponding data is given in Table 5.

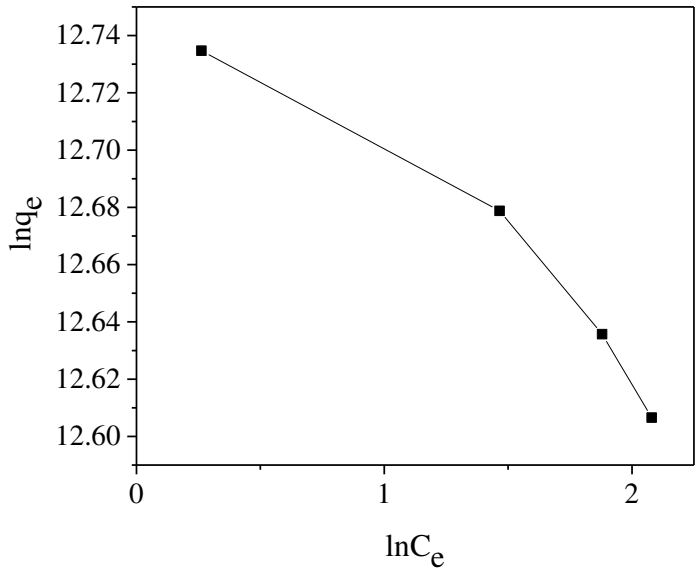

311

312 Fig. 8 Freundlich plot of SO_2 adsorption on AC-4

313 *4.3 D-R isotherm*

314 Fig. 9 shows the plot of $\ln C_{ads}$ vs ε^2 for adsorption data of toxic gas on AC-4 surface at initial
315 concentration of 57 ppm and 298 K. From intercept and slope of plot we get value of D-R
316 parameters (Sumathi, Bhatia et al. 2010). R^2 value provides information about the favorability of
317 adsorption process. Fig. 9 shows D-R isotherm plot and its corresponding data is given in Table 5.

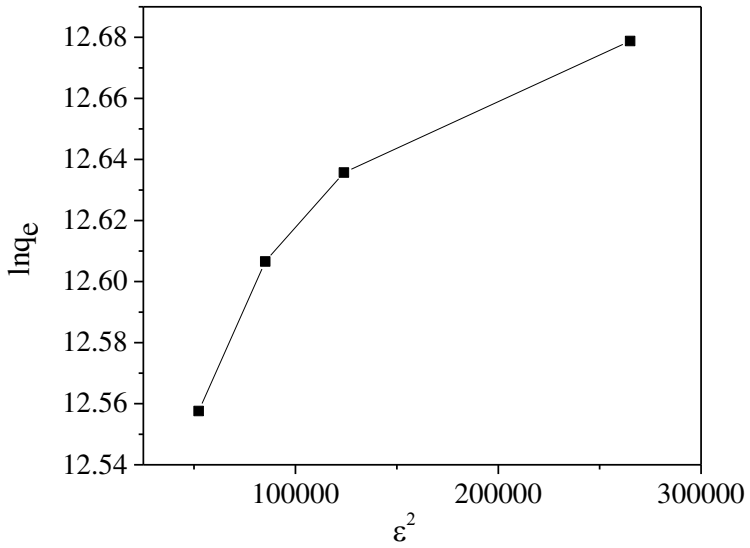

Fig. 9 D-R plot of SO_2 adsorption on AC-4

5. Adsorption Kinetics

Plot of log (q_e-q_t) vs t for pseudo first order reaction is shown in Fig. 10 and plot of t/q_t vs T for pseudo second order reaction is shown in Fig. 11 for the adsorption of SO_2 gas on AC-4. Kinetics of adsorption can be predicted from the corresponding value of R^2 (Yi, Wang et al. 2014). Value of R^2 for pseudo first order reaction is 0.7223 and for second order is 1. This concludes that pseudo second order reaction is the most favorable path for adsorption of SO_2 on AC-4 and fits best to adsorption process (Sumathi, Bhatia et al. 2010).

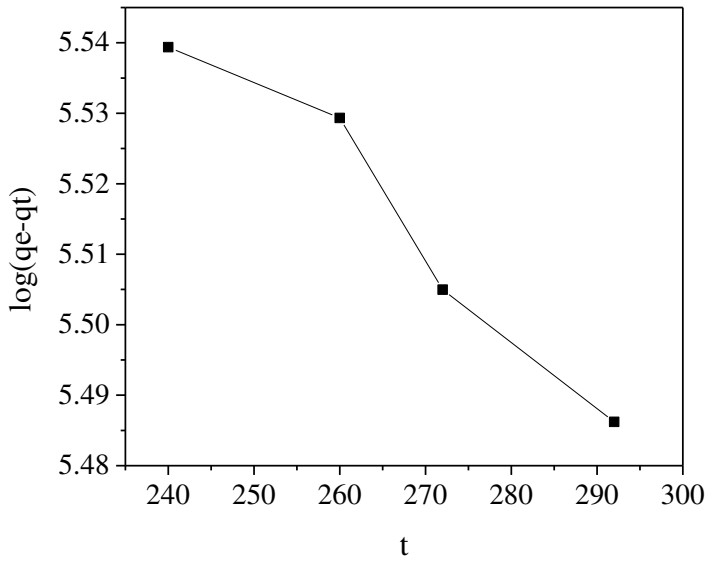

328

329 Fig. 10 Plot of pseudo first order for SO_2 adsorption on AC-4

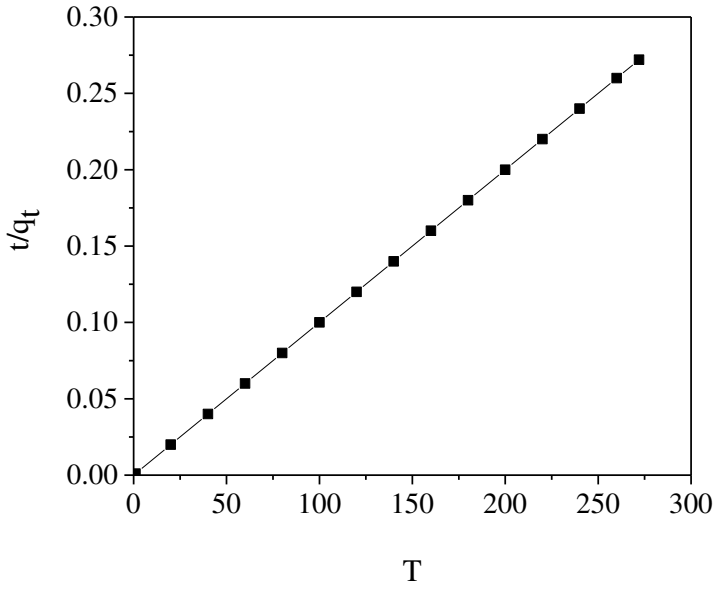

330

331 Fig. 11 Plot of pseudo second order for SO_2 adsorption on AC-4

332 **6. Thermodynamic parameters**

333 Plot of $\ln K_d$ vs 1/T is shown in Fig. 12. From the slope and intercept of this graph value of ΔG and
334 ΔH have been computed respectively. Positive value of ΔS proposed an increased randomness at
335 the interface in the adsorption process. Positive enthalpy value shows the endothermic reaction
336 while negative free energy indicates the spontaneous nature of adsorption process respectively
337 (Zhou, Yi et al. 2012). Corresponding values are shown in Table 5. Comparison of three isotherm
338 models shows that Langmuir adsorption isotherm model is the best fitted model as compared to
339 Freundlich and D-R isotherms.

340

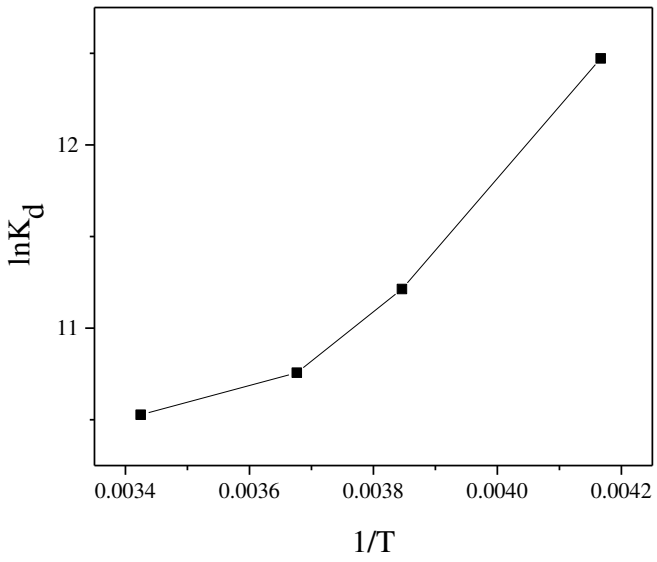

341 Fig. 12 Plot of lnKd vs 1/T for thermodynamic parameters

342 Table 5 Parameters for Langmuir, Freundlich and D-R isotherms for SO_2 adsorption

Gas adsorbed	Models	Parameters		ΔH ($kJmol^{-1}$)	ΔS ($JK^{-1}mol^{1}$)	ΔG ($kJmol^{-1}$)
SO_2	Langmuir	Q	0.017	6628.2	9.42	-26.08
		B	0			
		R^2	1			
	Freundlich	K_f	12.7			
		1/n	-0.057			
		R^2	0.941			

	q_s	2.5
D-R	K_D	5×10^{-7}
	R^2	0.864

Conclusion

In this study different TEDA impregnated ACs were prepared by using sublimation method. All samples displayed higher breakthrough times and gas adsorption capacities to a considerable amount as compared to the Raw AC. Moreover, AC-4 prepared in this work is a sustainable candidate for the purification of toxic gases from contaminated air by chemisorption on porous carbon surface. Its breakthrough time and adsorption capacity was found to be 264 minutes and 3.74gSO_2/g-C respectively for 57 ppmv SO_2. Being basic in nature, TEDA played a dynamic role in the purification of acidic gases from air. Gas adsorption data are reliable with Langmuir, Freundlich and D-R isotherms. Adsorption data strongly follow Langmuir adsorption isotherm and pseudo second order kinetics. Thermodynamic parameters ΔH, ΔG and ΔS have been calculated. However the positive enthalpy change showed the endothermic reaction for adsorption of SO_2 on AC. While negative free energy change confirmed the spontaneous nature of adsorption process.

Ethics approval and consent to participate

Not applicable

Consent for publication

Not applicable

Availability of data and materials

Not applicable

Declaration of competing interest

362 The authors declare no competing financial interest.

363 **Funding**

364 This research did not receive any specific grant from funding agencies in the public, commercial
365 or not-for-profit sectors.

366 **Author contribution**

367 Sidra Shaoor Kiani: Literature review, Writng original manuscript

368 Atif Ullah: Experimentation

369 Amjad Farooq: Reagents and other analysis tools, Methodology, Validation, Investigation,
370 Formal analysis, Reviewing manuscript

371 Naseem Irfan: Instrumentation

372 Masroor Ahmed: Instrumentation

373 Mohsan Nawaz: Conceptualization

374 **References**

375 Abdulrasheed, A., et al. (2018). "Surface modification of activated carbon for adsorption of SO2
376 and NOX: A review of existing and emerging technologies." Renewable and Sustainable Energy
377 Reviews **94**: 1067-1085.

378 American Society for Testing and Materials (ASTM) Refractories, Carbon and Graphite Products;
379 Activated Carbons,. (1996). West Conshohocken.

380 Al-Qodah, Z. and R. Shawabkah (2009). "Production and characterization of granular activated
381 carbon from activated sludge." Brazilian Journal of Chemical Engineering **26**(1): 127-136.

382 Arcibar-Orozco, J. A., et al. (2013). "Reactive adsorption of SO2 on activated carbons with
383 deposited iron nanoparticles." Journal of Hazardous Materials **246**: 300-309.

384 Bobbitt, N. S., et al. (2017). "Metal–organic frameworks for the removal of toxic industrial
385 chemicals and chemical warfare agents." Chemical Society Reviews **46**(11): 3357-3385.

386 Cai, Y., et al. (2021). "Hydrothermal-ultrasonic synthesis of CuO nanorods and CuWO4
387 nanoparticles for catalytic reduction, photocatalysis activity, and antibacterial properties."
388 Materials Chemistry and Physics **258**: 123919.

389 Eskandari, L., et al. (2020). "Facile colorimetric detection of Hg (II), photocatalytic and
390 antibacterial efficiency based on silver-manganese disulfide/polyvinyl alcohol-chitosan
391 nanocomposites." International Journal of Biological Macromolecules **164**: 4138-4145.

392 Farooq, A., et al. (2012). Impregnation of TEDA onto Activated Carbon at Pilot Scale Level.

393 González-García, C., et al. (2011). "Removal efficiency of radioactive methyl iodide on TEDA-
394 impregnated activated carbons." Fuel processing technology **92**(2): 247-252.

395 Ho, K., et al. (2019). "Design of highly efficient adsorbents for removal of gaseous methyl iodide
396 using tertiary amine-impregnated activated carbon: Integrated experimental and first-principles
397 approach." Chemical Engineering Journal **373**: 1003-1011.

398 Ho, K., et al. (2019). "Adsorptive removal of gaseous methyl iodide by triethylenediamine
399 (TEDA)-metal impregnated activated carbons under humid conditions." Journal of Hazardous
400 Materials **368**: 550-559.

401 Huve, J., et al. (2018). "Porous sorbents for the capture of radioactive iodine compounds: a
402 review." RSC advances **8**(51): 29248-29273.

403 Hyuncheol Lee, K. K., Dooyong Lee, Haksu Kim, Chorong Kim (2019). "The Effect of Toxic
404 Gases on TEDA Impregnated Activated Carbon." **2019**: 420-420.

405 Khayan, K., et al. (2019). "Active carbon respiratory masks as the adsorbent of toxic gases in
406 ambient air." Journal of toxicology **2019**.

407 Kiani, S. S., et al. (2020). "Synthesis and adsorption behavior of activated carbon impregnated
408 with ASZM-TEDA for purification of contaminated air." Diamond and Related Materials: 107916.

409 Kiani, S. S., et al. (2021). "Investigation of Cu/Zn/Ag/Mo-based impregnated activated carbon for
410 the removal of toxic gases, synthesized in aqueous media." Diamond and Related Materials **111**:
411 108179.

412 Lee, H. C., et al. (2020). "Performance evaluation of TEDA impregnated activated carbon under
413 long term operation simulated NPP operating condition." Nuclear Engineering and Technology.

414 Lodewyckx, P., et al. (2004). "The Wheeler–Jonas equation: a versatile tool for the prediction of
415 carbon bed breakthrough times." Carbon **42**(7): 1351-1355.

416 Lua, A. C. and J. Guo (2001). "Adsorption of sulfur dioxide on activated carbon from oil-palm
417 waste." Journal of Environmental Engineering **127**(10): 895-901.

418 Mahle, J. J., et al. (2010). "Role of TEDA as an activated carbon impregnant for the removal of
419 cyanogen chloride from air streams: synergistic effect with Cu (II)." The Journal of Physical
420 Chemistry C **114**(47): 20083-20090.

421 Muzarpar, M. S., et al. (2020). "The Adsorption Mechanism of Activated Carbon and Its
422 Application-A Review." International Journal of Advanced Technology in Mechanical,
423 Mechatronics and Materials **1**(3): 118-124.

424 Myers, A. (2002). "Thermodynamics of adsorption in porous materials." AIChE journal **48**(1):
425 145-160.

426 Perera, M. S. A., et al. (2012). "Estimation of gas adsorption capacity in coal: a review and an
427 analytical study." International Journal of Coal Preparation and Utilization **32**(1): 25-55.

428 Sumathi, S., et al. (2010). "Adsorption isotherm models and properties of SO2 and NO removal
429 by palm shell activated carbon supported with cerium (Ce/PSAC)." Chemical Engineering Journal
430 **162**(1): 194-200.

431 Wen, J., et al. (2021). "Bimetal cobalt-Iron based organic frameworks with coordinated sites as
432 synergistic catalyst for fenton catalysis study and antibacterial efficiency." Colloids and Surfaces
433 A: Physicochemical and Engineering Aspects **610**: 125683.

434 Wu, L.-C., et al. (2007). "Removal of hydrogen sulfide and sulfur dioxide by carbons impregnated
435 with triethylenediamine." Journal of the Air & Waste Management Association **57**(12): 1461-
436 1468.

437 Yang, M., et al. (2020). "Biosynthesis of nano bimetallic Ag/Pt alloy from Crocus sativus L.
438 extract: biological efficacy and catalytic activity." Journal of Photochemistry and Photobiology B:
439 Biology **212**: 112025.

440 Yi, H., et al. (2014). "Adsorption of SO2, NO, and CO2 on activated carbons: equilibrium and
441 thermodynamics." Journal of Chemical & Engineering Data **59**(5): 1556-1563.

442 Zhou, C., et al. (2011). "A simple method for calculating the overall adsorption rate constant in
443 the Wheeler–Jonas equation." Adsorption Science & Technology **29**(1): 71-82.

444 Zhou, J., et al. (2014). "Study on adsorption performance of coal based activated carbon to
445 radioactive iodine and stable iodine." Annals of Nuclear Energy **72**: 237-241.

446 Zhou, X., et al. (2018). "Capture of pure toxic gases through porous materials from molecular
447 simulations." Molecular Physics **116**(15-16): 2095-2107.

448 Zhou, X., et al. (2012). "Thermodynamics for the adsorption of SO2, NO and CO2 from flue gas
449 on activated carbon fiber." Chemical Engineering Journal **200**: 399-404.